https://doi.org/10.1016/j.dyepig.2021.109623

Self-assembled flexible metallo-supramolecular film based on Fe(II) ion and triphenylamine-subsituted alkyl terpyridine towards electrochromic application

Yu Kuai,[a] Tao Yang,[a] Feiya Yuan,[a] Yujie Dong,*[a] Qingbao Song,[a] Cheng Zhang*[a] and Wai-Yeung Wong*[b,c]

[a] College of Chemical Engineering, Zhejiang University of Technology, Chaowang Road, Hangzhou 310014, P. R. China. E-mail: dongyujie@zjut.edu.cn; czhang@zjut.edu.cn
[b] Department of Applied Biology & Chemical Technology, The Hong Kong Polytechnic University, Hung Hom, Hong Kong, P. R. China. E-mail: wai-yeung.wong@polyu.edu.hk.
[c] Hong Kong Polytechnic University Shenzhen Research Institute, Shenzhen 518057, P. R. China.

Abstract

A new metallo-supramolecular film was prepared by a liquid–liquid interface self-assembly method based on the metal ion Fe(II) in water solution and a star-shaped ligand of triphenylamine-substituted alkyl terpyridine in organic solvents. The film obtained exhibited excellent flexibility due to the presence of flexible alkyl arms, and could tightly adhere to the surface of ITO glass with very smooth surface morphology via SEM characterization. Spectroelectrochemical experiments demonstrated that the film displayed the electrochromism with purplish color in the neutralized state at 0 V vs Ag/AgCl turning to yellow-green color in the oxidized state at 1.2 V vs Ag/AgCl. This work further indicates that the liquid–liquid interfaciad self-assembly method is a promising strategy to prepare the metallo-supramolecular film towards electrochromic applications.

Keywords self-assembly, metallo-supramolecular film, electrochromism, terpyridine, triphenylamine

1. Introduction

In the past decades, the electrochromic (EC) materials have been investigated extensively because of their potential application in reflecting mirrors, electronic skin, flat-panel display, smart windows and so on[1-9]. For EC applications, the materials are usually prepared as a uniform thin film on ITO electrode, generally by electrochemical polymerization, spray/spin-coating or evaporation/sputtering methods[10-17]. However, electropolymerization has high requirements for monomers as well as spray/spin-coating. The monomers for electropolymerization and solution-processing need electroactive sites and good solubility, respectively. Sputtering methods only adapt to the inorganic materials, while the evaporation method is difficult to be widely used in commercial electrochromic field because of its high cost of instruments and it is also limited to the small organic matter or some inorganic materials[18-25]. Therefore, exploration of new film forming methods for electrochromic materials is of great significance.

Recently, the liquid/liquid interfacial self-assembly between metal ions dissolved in aqueous solution and ligand dissolved in organic solution, has emerged as a new method to prepare the electrochromic film materials, in which metal ions and ligands meet at the interface between aqueous phase and organic phase to form a thin film via the coordination interaction. The terpyridine derivatives have been widely adopted as the ligand, and Fe(Ⅱ), Co(Ⅱ) and Ni(Ⅱ) ions are usually the metal ions[26-29]. The strong coordination interaction force makes the final thin film at the interface to be a

highly stable one, and suitable combination of metal ions and ligand will enable the film obtained with desired optical and electrical properties[30-35]. Some reported metallo-supramolecular films seem to be fragile and not easy to be transferred and processed, possibly due to the strong rigidity of the ligand structure[36-39]. A simple idea is that a flexible metallo-supramolecular films might be obtained through the adjustment of the rigidity of the ligand structure via the liquid/liquid interfacial self-assembly method.

In this work, a new star-shaped molecular structure (**TBT**) with triphenylamine as the central core and tripyridine as the three arms was designed and synthesized, but the central core and arms are linked with butamethylene fragment to break the conjugation between terphenylamine and tripyridine structures, which is expected to increase the flexibility of the metallo-supramolecular films by introducing flexible alkyl chains. The corresponding metallo-supramolecular film (**TBT-Fe**) was successfully fabricated on the ITO surface directly. The film obtained exhibited excellent flexibility, and displayed very smooth surface morphology. After applying different voltages, the TBT-Fe films finally exhibited obvious electrochromism.

2. Experimental

2.1 Materials and instruments

Reagents and solvents used in the synthesis and characterization were purchased from J&K, Aladdin, Energy Chemical, Admas and Bidepharm, and used without further purification if not specified. The spectroelectrochemistry tests (optical contrast,

switching time) were investigated by Shimadzu UV-1800 spectrophotometer (Shimadzu, Japan) integrated with the CHI660E electrochemical workstation in a three-compartment system containing 0.1M Bu_4NClO_4 in acetonitrile solution. The morphology of films was tested using a Hitachi S-4800 scanning electron microscope (Hitachi, Japan). The structure investigation of the synthesized compounds were recorded by AVANCE Ⅲ HD NMR (Bruker, Switzerland) and autoflex maX MALDI-TOF(TOF) (Bruker, Switzerland).

2.2 Synthesis of ligand

Synthesis of **tris(4'-methoxy-[1, 1'-biphenyl]-4-yl)amine** (**1**)

Tri(4-bromophenylamine) (0.48 g, 1 mmol) and *p*-methoxyphenylboric acid (0.53 g, 3.5 mmol) were stirred in ethylene glycol diethyl ether (30 ml), followed by the addition of tetrakis(triphenylphosphine)palladium (0.12 g, 0.1 mmol). The reaction mixture was quickly heated to reflux and stirred in N_2 for 24 h. After cooling to room temperature, the reaction mixture was poured into 100 ml deionized water and extracted with dichloromethane. The organic phase was dried by magnesium sulfate and evaporated. The crude product was purified by column chromatography on a silica gel with dichloromethane/hexane (1:3, v/v) to yield a white solid (0.5 g, 90%). ^{1}H NMR (500 MHz, $CDCl_3$) δ 7.54 (d, J = 8.8 Hz, 6H), 7.49 (d, J = 8.7 Hz, 6H), 7.23 (d, J = 8.7 Hz, 6H), 6.99 (d, J = 8.8 Hz, 6H), 3.87 (s, 9H). ESI HRMS (mass m/z): found: 564.2518 [M^+ + H] (calculated: 564.2533).

Synthesis of **4', 4''', 4''''''-nitrilotris(([1, 1'-biphenyl]-4-ol))** (**2**)

Compound **1** (0.56 g, 1 mmol) was stirred in dichloromethane (30 ml), followed by

the addition of a boron tribromide solution of dichloromethane (1 mol/L, 3 mL, 3 mmol) dropwise. After the reaction mixture was stirred at room temperature for 12 h, the reaction mixture was poured into deionized water (100 ml) and extracted with dichloromethane. The organic phase was dried by magnesium sulfate and evaporated. The crude product was purified by column chromatography on a silica gel with dichloromethane to yield a white solid (0.42 g, 80%). ^{1}H NMR (500 MHz, DMSO-d_6) δ 9.49 (s, 3H), 7.54 (d, *J* = 8.7 Hz, 6H), 7.47 (d, *J* = 8.6 Hz, 6H), 7.10 (d, *J* = 8.6 Hz, 6H), 6.83 (d, *J* = 8.8 Hz, 6H). ESI HRMS (mass m/z): 522.2053 [M^+ + H] (calculated: 522.2064).

Synthesis of **4'-(4-methoxyphenyl)-2, 2': 6', 2"-terpyridine** (**3**)

1, 4-Dibromobutane (1.3 g, 6 mmol) and potassium carbonate (0.48 g, 3.5 mmol) were stirred in acetone (30 ml), followed by the addition of compound **2** (0.52 g, 1 mmol). The reaction mixture was heated up to reflux and stirred under N_2 for 24 h. After cooling to room temperature, the reaction mixture was poured into 100 ml deionized water and extracted with dichloromethane. The organic phase was dried by magnesium sulfate and evaporated. The crude product was purified by column chromatography on a silica gel with dichloromethane/hexane (1:2, v/v) to yield a white solid (0.46 g, 50%). ^{1}H NMR (500 MHz, $CDCl_3$) δ 7.53 (d, *J* = 8.7 Hz, 6H), 7.49 (d, *J* = 8.8 Hz, 6H), 7.22 (d, *J* = 8.6 Hz, 6H), 6.97 (d, *J* = 8.8 Hz, 6H), 4.07 (t, *J* = 6.3 Hz, 6H), 3.53 (t, *J* = 6.4 Hz, 6H), 2.15 – 2.09 (m, 6H), 2.02 - 1.97 (m, 6H). ESI HRMS (mass m/z): 924.1227 [M^+ + H] (calculated: 924.1257).

Synthesis of **([2, 2': 6', 2"-terpyridin]-4'-yl)phenol** (**4**)

p-Methoxybenzaldehyde (0.14 g, 1 mmol), potassium hydroxide (0.14 g, 2.5 mmol) and 2-acetylpyridine (0.3 g, 2.5 mmol) were stirred in ethanol (30 ml), followed by the addition of ammonium hydroxide (30 ml). After stirring for 24 h at room temperature, the greyish-green solid was precipitated. The precipitate was filtered and washed using tetrahydrofuran and then the crude product was purified by recrystallization with ethanol to yield an orange solid (0.27g, 80%). ^{1}H NMR (500 MHz, $CDCl_3$) δ 8.75 (d, *J* = 4.3 Hz, 2H), 8.73 (s, 2H), 8.69 (d, *J* = 7.9 Hz, 2H), 7.91 – 7.87 (m, 4H), 7.37 (dd, *J* = 6.5, 4.8 Hz, 2H), 7.05 (d, *J* = 8.8 Hz, 2H), 3.91 (s, 3H). ESI HRMS (mass m/z): 340.1435 [M^+ + H] (calculated: 340.1444).

Synthesis of **tris(4'-(4-bromobutoxy)-[1, 1'-biphenyl]-4-yl)amine** (**5**)

Compound **4** (0.34 g, 1 mmol) and pyridine hydrochloride (2.3 g, 20 mmol) were added into a 10 mL reaction tube. The reaction mixture was heated up to 180 ℃ and stirred under N_2 for 24 h. After cooling to room temperature, the reaction mixture was poured into deionized water (10 ml) and filtered. The residue was washed using deionized water and dried to yield a brown solid (0.1g, 30%). ^{1}H NMR (500 MHz, DMSO-d_6) δ 8.91-8.84 (m, 4H), 8.79 (s, 2H), 8.32 – 8.25 (m, 2H), 7.91 (d, *J* = 8.6 Hz, 2H), 7.78 – 7.69 (m, 2H), 7.00 (d, *J* = 8.7 Hz, 2H). ESI HRMS (mass m/z): 326.1294 [M^+ + H] (calculated: 326.1288).

Synthesis of **tris(4'-(4-(4-([2,2':6',2''-terpyridin]-4'-yl)phenoxy)butoxy)-[1,1'-biphenyl]-4-yl)amine** (**TBT**)

Compound **3** (0.92 g, 1 mmol) and compound **5** (1.3 g, 4 mmol) were stirred in N-dimethylformamide (30 ml) under N_2, followed by the addition of potassium

carbonate (0.62 g, 4.5 mmol). The reaction mixture was heated up to 80 ℃ and stirred under N_2 for 24 h. After cooling to room temperature, the reaction mixture was poured into deionized water (100 ml) and filtered. The residue was washed using ethyl alcohol and dried to yield a brown solid (0.58g, 35%). ^{1}H NMR (500 MHz, $CDCl_3$) δ 8.84 – 8.77 (m, 12H), 8.75 (d, *J* = 8.0 Hz, 6H), 8.01 – 7.91 (m, 12H), 7.54 (d, *J* = 8.7 Hz, 6H), 7.49 (d, *J* = 8.6 Hz, 6H), 7.46 – 7.40 (m, 6H), 7.22 (d, *J* = 8.6 Hz, 6H), 7.06 (d, *J* = 8.6 Hz, 6H), 7.00 (d, *J* = 8.7 Hz, 6H), 4.20 - 4.10 (m, 12H), 2.12 - 2.02 (m, 12H). MALDI-TOF MS (mass m/z): 1659.8082 [M] (calculated: 1659.8073). ^{13}C NMR (600MHz, $CDCl_3$) δ 160.04, 158.20, 156.03, 155.47, 149.87, 148.80, 146.30, 137.17, 135.14, 130.47, 128.58, 127.71, 127.40, 124.37, 123.87, 121.57, 118.51, 114.87, 67.59, 26.06. Melting point: 110±5 ℃.

Preparation of the films TBT-Fe

The 50 ml of aqueous solution of $Fe(BF_4)_2 \cdot 6H_2O$ (50 mM) was added into a watch glass and then ITO glass was also put into the solution. A 0.10 mM solution of **TBT** was prepared by dissolving **TBT** (1.7 mg, 0.001 mmol) in 10 ml dichloromethane solution. The solution of **TBT** (0.5 ml) was injected onto the glass surface with a syringe. The film emerged at the interface between aqueous solution and dichloromethane solution along with the dichloromethane solvents volatilized, and attached onto the ITO glass eventually. The ITO with the film attached would be immersed into deionized water, ethyl alcohol and dichloromethane in sequence to remove $Fe(BF_4)_2$ and **TBT**.

3. Results and discussion

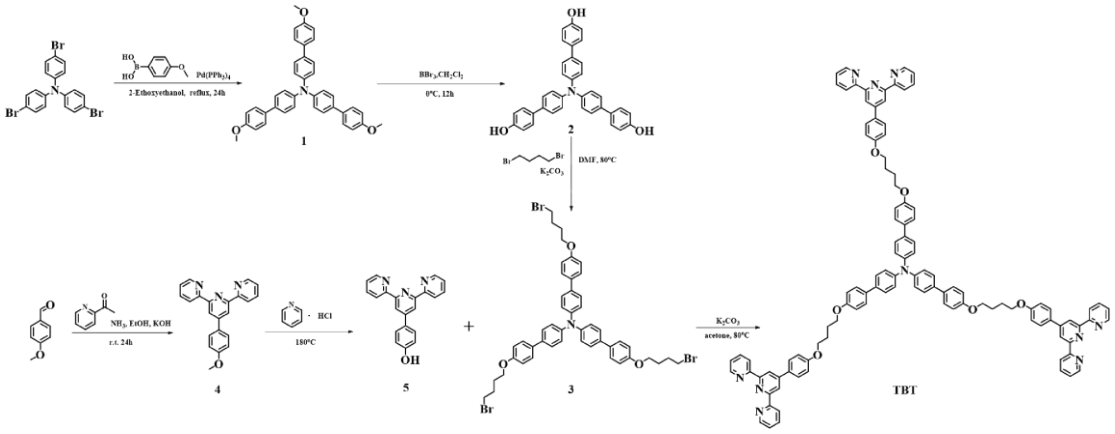

Scheme.1 The synthesis route of ligand molecule **TBT**.

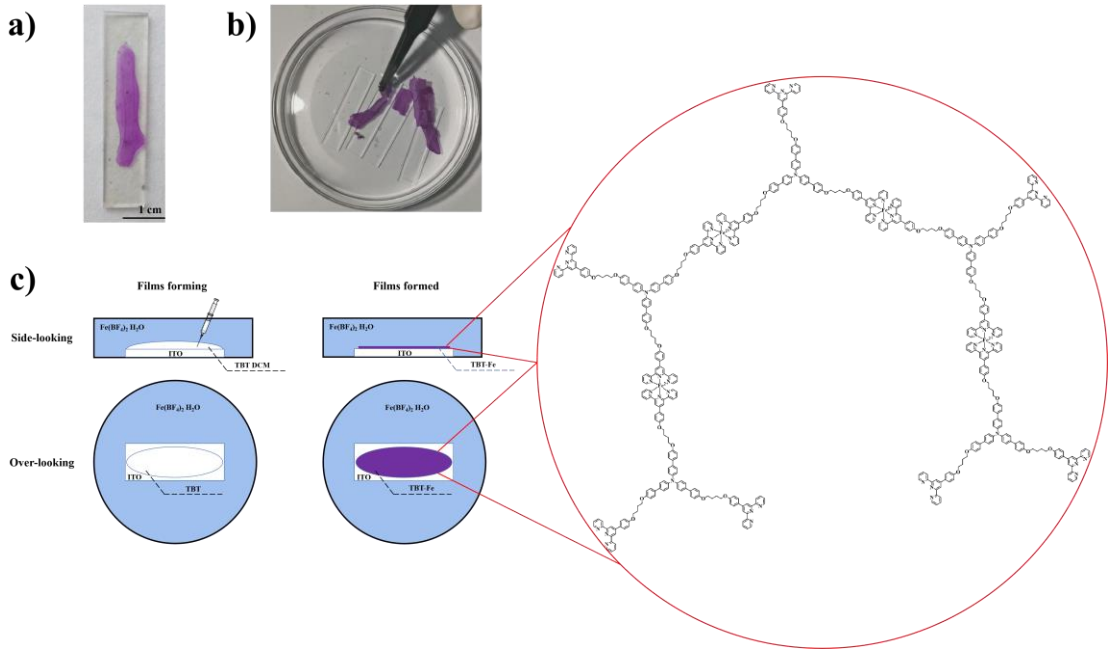

Fig.1 a) The prepared **TBT-Fe** film adhering on the ITO glass. b) The photo of flexible film finally generated in water via liquid-liquid interfacial self-assembly method. c) The scheme of preparation process of liquid-liquid interfacial self-assembly method and the molecular structure of the metallo-supramolecular film.

The synthesis route of the star-shaped molecule **TBT** is shown in Scheme. 1 and the experimental detail for the synthesis has been described in the experimental part. NMR and mass spectral characterization prove the successful acquisition of the

molecular structure of **TBT**. The corresponding metallo-supramolecular film of **TBT-Fe** was then prepared by the liquid-liquid interfacial self-assembly method at the interface between the aqueous phase of $Fe(BF_4)_2$ in water and the organic phase of **TBT** in dichloromethane. Due to the very good solubility of **TBT**, the insoluble film of **TBT-Fe** could not be formed at the interface initially. The preparation method was improved by injecting the dichloromethane solution (0.5 ml) of **TBT** (0.1 mmol/L) to the ITO glass surface which had been put in the aqueous solution of $Fe(BF_4)_2$ (50 mmol/L) as shown in Fig. 1c. The **TBT-Fe** film would appear at the interface between aqueous and organic phases gradually, and eventually adhere on the surface of ITO along with the dichloromethane solvent totally volatilized after several days. By this method, **TBT-Fe** films were obtained directly on the surface of ITO glass without the additional transference process (Fig. 1a).

It was surprising that the final **TBT-Fe** films exhibited highly flexible property, which could be dragged and pulled by tweezers on the surface of aqueous solution without easily down as shown in Fig. 1b. Considering the flexible alkyl chain in the ligand structure of **TBT** and in comparison to the reported relatively fragile metallo-supramolecular film with a rigid ligand structure[40], the flexibility of **TBT-Fe** was supposed to be mainly ascribed to the introduction of alkyl chains. This indicated that it is possible to obtain the corresponding property we desired for metallo-supramolecular films by modifying the ligand structure.

The surface morphology of the **TBT-Fe** films adhering to the ITO glass was further evaluated by scanning electron microscopy (SEM). It was found that the

TBT-Fe film showed a smooth surface morphology as shown in Fig 2a. Some small round pits were observed at the surface of film, and it was thought to be caused by the bubbles owing to the volatilization of dichloromethane solvent in the film forming process. As shown in Fig 2b, the multi-layer film structure was observed at the edge of **TBT-Fe** films, which might indicate the layer growth model of metallo-supramolecular film, corresponding with the growth of film as the volatilization of dichloromethane solvents gradually. Energy dispersive spectroscopy (EDS) was also used to evaluate the composition of **TBT-Fe** films and the results were listed in Table 1. It was found that the atomic percentages of N and Fe were measured to be 1.19% and 0.20% respectively. The calculated ratio of N/Fe was nearly 6/1, very close to the ideal ratio of 6.6/1 in the metal complex structure of **TBT-Fe** films. These results indicated the successful fabrication of **TBT-Fe** films through the liquid-liquid interfacial self-assembly of Fe(Ⅱ) metal ions and **TBT** ligand molecules. IR spectrum showed the peak at about 1584 cm^{-1} which belongs to the C=C stretching vibration of **TBT** which shifted to 1602 cm^{-1} in **TBT-Fe**, indicating that terpyridyl ligand is coordinated to the metal ion. In addition, the peak at around 1090 cm^{-1} should be attributed to BF_4^-[30].

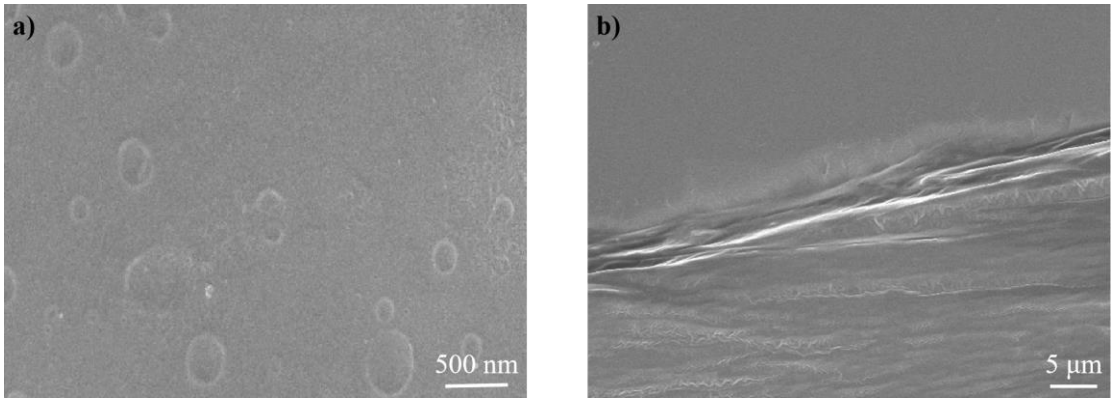

Fig.2 The SEM image of body (a) and edge (b) of the **TBT-Fe** film on ITO glass.

Table 1 The EDS data of the **TBT-Fe** films.

element	C	N	O	F	Si	Fe	In	Sn
Atomic percent	63.54%	1.19%	11.74%	5.61%	7.81%	0.20%	8.16%	1.12%

The UV-Vis absorption spectra of **TBT-Fe** films were also characterized as shown in Fig. 3. A stinging absorption peak at about 570 nm and a wide absorption peak at about 350 nm were observed. **TBT** ligand exhibited an obvious absorption peak at about 350 nm in the UV-Vis absorption spectra. It was obvious that the absorption peak at 570 nm in the UV-Vis absorption spectra of **TBT-Fe** films was newly generated with an obvious redshift of about 220 nm in comparison to that of **TBT** ligand, which should be attributed to the metal-to-ligand charge transfer transition of the Fe(Ⅱ)-terpyridine group and well consistent with those data of the reported Fe(Ⅱ)-terpyridyl coordination compounds. Thus the UV spectra indicated the successful fabrication of **TBT-Fe** films through the liquid-liquid interfacial self-assembly of Fe(Ⅱ) metal ions and **TBT** ligand molecule.

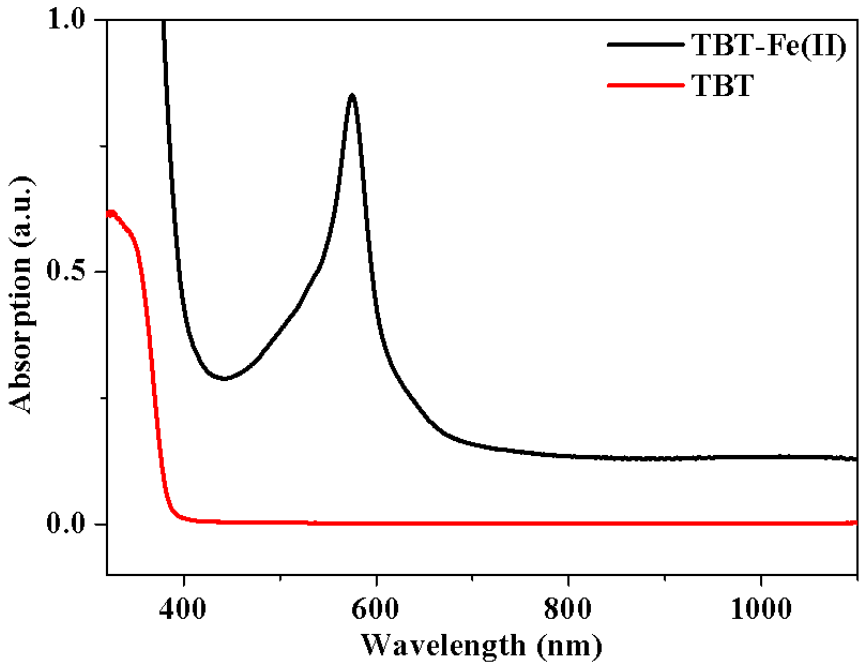

Fig.3 The UV-Vis absorption spectra of **TBT-Fe** film and **TBT** ligand in solution.

The cycle voltammogram curve of **TBT-Fe** films was carried out in a three-compartment system containing the ITO glass with **TBT-Fe** films as the working electrode, Ag/AgCl as the reference electrode, platinum wire as the counter electrode, and 0.1 M Bu_4NClO_4 in acetonitrile solution as the electrolyte. As shown in Fig 4, there were two pairs of redox peaks at about 0.9/0.75 V and 1.2/1.0 V, respectively, which should be attributed to the redox behavior of central triphenylamine and Fe(Ⅱ)-terpyridyl groups respectively. In comparison to the similar Fe(Ⅱ)-terpyridyl derivant which had reported[40,41], the redox potential of Fe(Ⅱ)-terpyridyl groups of **TBT-Fe** film was semblable, while that of triphenylamine group was lower obviously, which might be ascribed to the breaking in the linkage of the electron-withdrawing Fe(Ⅱ)-terpyridyl groups to the triphenylamine group owing to the alkyl chain.

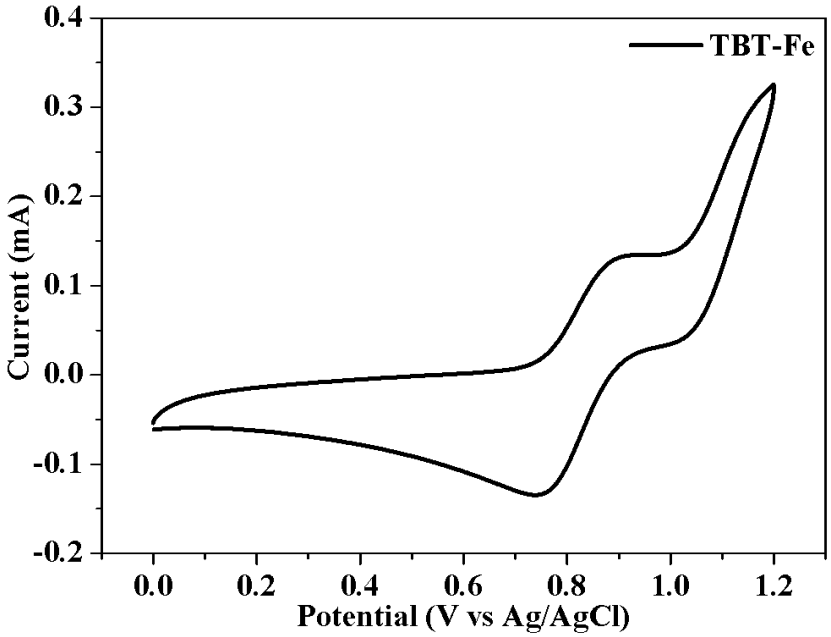

Fig.4 The cycle voltammogram curve of the **TBT-Fe** films with the applied potential between 0 to 1.2 V at a scanning rate of 0.1 V s^{-1} with a three-compartment system containing 0.1 M Bu_4NClO_4 in acetonitrile solution as the electrolyte.

The electrochromic properties of **TBT-Fe** films were determined by spectroelectrochemical experiments. As shown in Fig. 5, the **TBT-Fe** films displayed a purple color in the neutral state at 0 V, with the maximum absorption peak located at about 570 nm. When the applied voltage of **TBT-Fe** films was increased from 0 V vs Ag/AgCl to 1.0 V vs Ag/AgCl, a new and wider absorption peak appeared in the range of 700-1100 nm in the absorption spectra, which was consistent with the absorption peak of oxidized triphenylamine groups according to the reported literature. It further proved that the redox peaks at 0.9/0.75 V vs Ag/AgCl in the cyclic voltammetry curve was attributed to that of the triphenylamine group in the **TBT-Fe** films. The film color did not change much at 1.0 V vs Ag/AgCl due to the change of absorption almost located at the range of invisible spectral range. When the applied

voltage was further increased from 1.0 to 1.2 V vs Ag/AgCl, the absorption peak of **TBT-Fe** films at 570 nm is reduced obviously and almost disappears finally, accompanied with the film color changed from original purple color in the neutral state to yellow-green color in the oxidized state. Such a transformation of absorption spectra was very similar to that of the reported coordinated terpyridine-Fe(Ⅱ) groups[30], which proved that the redox peak at 1.2 V/1.0 V vs Ag/AgCl in the cyclic voltammetry curve was supposed to be attributed to the redox behavior of the coordinated terpyridine-Fe(Ⅱ) group in the **TBT-Fe** films. Therefore, it is obvious that the redox activity of the **TBT-Fe** films was composed of two redox processes, including the terpyridine-Fe(Ⅱ) group and the central triphenylamine group, both of which promote the electrochromic process of the **TBT-Fe** films to turn from purple to yellow-green color.

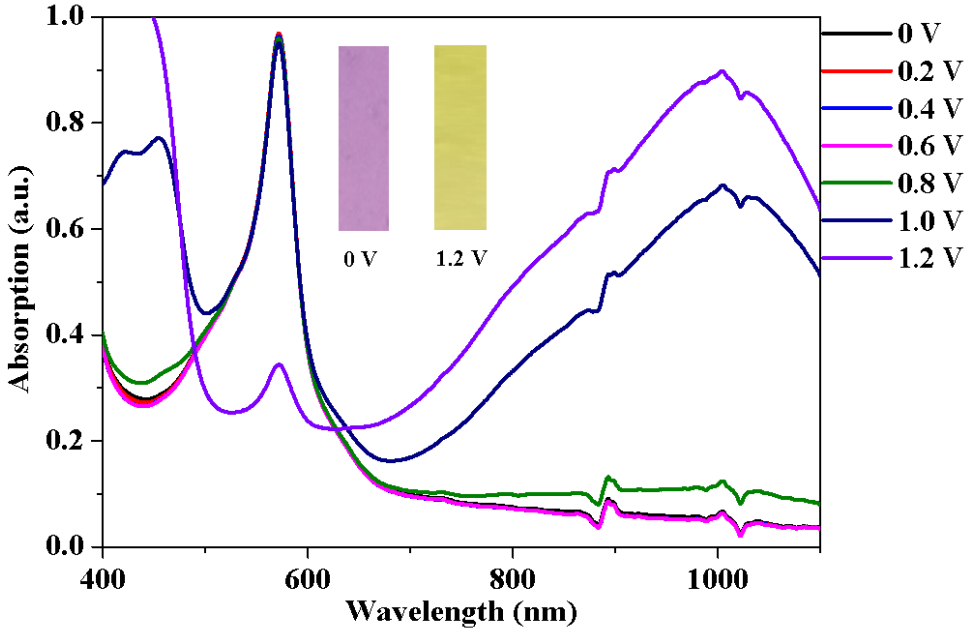

Fig.5 UV-vis absorption spectra of the **TBT-Fe** films with the applied potential from 0 V to 1.2 V vs Ag/AgCl in a solution of acetonitrile containing 0.1 M Bu_4NClO_4. Insets are the photos of

TBT-Fe films with the applied potentials at 0 V vs Ag/AgCl and 1.2 V vs Ag/AgCl.

The optical contrast and response time of **TBT-Fe** films were also measured under the repeated step voltages between 0 V vs Ag/AgCl and 1.2 V vs Ag/AgCl with the residence time set as 10 s and 15 s, respectively. As shown in Fig. 6a, the optical contrast of the **TBT-Fe** films at 570 nm is estimated to be about 20%. The switching time, which is calculated as the time required to achieve 95% of the full switch of the transmittance, was estimated to be about 14.3 s for coloring and 7.3 s for discoloring as shown in Fig. 6b and 6c, respectively. Compared with the response time of about 1 s of the previously reported **TPA-TPY-Fe** films, the response time is obviously larger in the case of **TBT-Fe** films. This is ascribed to the introduction of alkyl chain which could break the conjugation of ligand structure and thus decrease the charge transporting ability of TBT-Fe films.In addition, the coloration efficiency (CE) was also calculated with the equation CE = Δ OD/Q_d, and Δ OD = log(T_c/T_b), where T_c is the transmittance of oxidation, T_b is the transmittance of the neutral state, Q_d is the injected electronic charge in unit area. The CE of TBT-Fe is 172.82cm^2/C, which is close to most of other electrochromic materials reported [17,42].

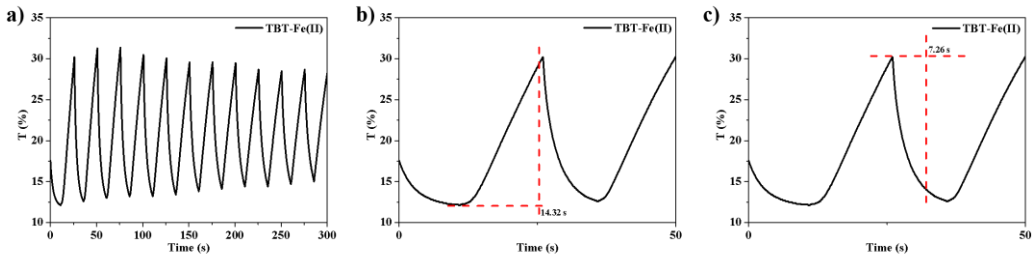

Fig.6 a) Optical contrast, response time of b) coloring and c) discoloring of the TBT-Fe films by applying the repeated step-potential with 0 V and 1.2 V vs Ag/AgCl at 570 nm.

A solid-state electrochromic device using **TBT-Fe** films as the electrochromic layer was fabricated with a double layer device structure as shown in Fig. 7a. Solid-state electrolyte was prepared from poly(methyl methacrylate) (PMMA) and lithium perchlorate, and it was sandwiched between a ITO glass adhering with **TBT-Fe** films and another blank ITO glass and further sealed to form the solid-state electrochromic device. The electrochromic device displayed an original purple color at 0 V which is in the neutral state, and the maximum absorption peak exists at about 570 nm (Fig.7b), which is the same as that of **TBT-Fe** film. When the applied voltage was increased to 3 V, a new and wider absorption peak appeared at 700-1100 nm, and at the same time, the original absorption peak at 570 nm decreased in intensity, accompanying with the device color changed from purple to yellow-green (Fig. 7b inset). The changes in colors and UV-vis spectra in electrochromic device were the same as those of **TBT-Fe** films measured in the electrochemical cell system.

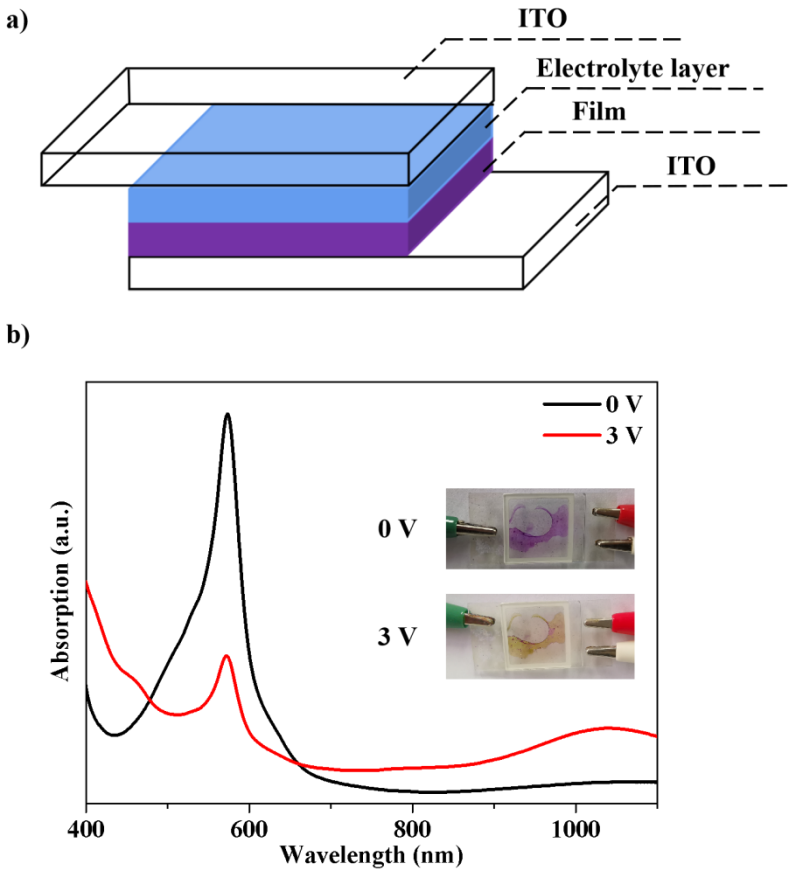

Fig.7 (a) The structure of the solid-state device. (b) UV-vis spectrum of the solid-state device with the applied potential from 0 V to 3.0 V. Insets are the photos of the solid-state device at 0 V and 3.0 V.

4. **Conclusion**

A flexible metallo-supramolecular film, a terpyridine-Fe(Ⅱ) complex **TBT-Fe**, was prepared based on the metal ion Fe(II) and a star-shaped ligand of triphenylamine-subsituted alkyl terpyridine via the liquid–liquid interfacial self-assembly method. The resulting metal-supramolecular films **TBT-Fe** exhibit excellent flexibility due to the presence of flexible arms containing alkyl chains. Obvious electrochromic behavior from purple to yellow-green color was observed for **TBT-Fe** film. The flexibility of ligand structure directly influences the flexible

property of the final metallo-supramolecular electrochromic materials. This work provides the possibility to prepare the flexible metallo-supramolecular films with obvious electrochromic performance via the liquid-liquid interfacial self-assembly method.

5. Acknowledgements

Thanks are given to the financial supports from National Natural Science Foundation of China (52073257, 51673083, 21875219, 52073242) and Zhejiang Provincial Natural Science Foundation of China (LY19E030006, LQ19E030016). W.-Y. W. would also like to thank the Hong Kong Research Grants Council (PolyU 153058/19P), Hong Kong Polytechnic University (1-ZE1C) and The Endowed Professorship in Energy from Ms. Clarea Au (847S) for the financial support.

6. References

[1] Zhang W, Li HZ, Hopmann E, Elezzabi A Y. Nanostructured inorganic electrochromic materials for light applications. *Nanophotonics,* **2020;** *10*(2): 825-850.

[2] Ma Q, Zhang H, Chen JX, Wu WW, Dong SJ. Lithium-ion-assisted ultrafast charging double-electrode smart windows with energy storage and display applications. *ACS Cent. Sci.*, **2020;** *6*: 2209-2216.

[3] Weng W, Higuchi T, Suzuki M, Fukuoka T, Shimomura T, Ono M, Radhakrishnan L, Wang HJ, Suzuki N, Oveisi H, Yamauchi *Y.* A High-speed passive-matrix electrochromic display using a mesoporous TiO_2 electrode with vertical porosity. *Angew. Chem. Int. Ed.*, **2010**; *49*: 3956-3959.

[4] Cai GF, Wang JX, Lee PS. Next-generation multifunctional electrochromic devices *Acc. Chem. Res*., **2016**; *49*: 1469-1476.

[5] Chang MJ, Chen WN, Xue HD, Liang DL, Lu XF, Zhou G. Conjugation-extended viologens with thiophene derivative bridges: near-infrared electrochromism, electrofluorochromism, and smart window applications *J. Mater. Chem. C*, **2020**; *8*: 16129-16142.

[6] Yu TH, Shao S, Yan Lj, Meng H, He YW, Yao C, Xu PP, Zhang XT, Hu WP, Huang W. Side-chain engineering of green color electrochromic polymer materials: toward adaptive camouflage application *J. Mater. Chem. C*, **2016;** *4*: 2269-2273.

[7] Malti A, Brooke R, Liu XJ, Zhao D, Ersman PA, Fahlman M, Jonsson MP, Berggren M, Crispin X. Freestanding electrochromic paper *J. Mater. Chem. C*, **2016**; *4*: 9680-9686.

[8] Malagon SS, Colin DR, Azizikhani H, Pellitero MA, Guirado G, Campo FJD. A self-powered skin-patch electrochromic biosensor *Biosens. Bioelectron.,* **2021**; *175*: 112879.

[9] Koo, J, Amoli V, Kim SY, Lee C, Kim J, Park S, Kim J, Ahn JM, Jung KJ, Kim DH. Low-power, deformable, dynamic multicolor electrochromic skin *Nano Energy*, **2020**; *78*: 105199.

[10] Keersmaecker MD, Reynolds JR. Simple interface modification of electroactive polymer film electrodes *ACS Appl. Mater. Interfaces,* **2019**; *11*: 47131—47142.

[11] Yagui J, Angel FA. Benzodithiophene-based small molecules for vacuum-processed organic photovoltaic devices *Opt. Mater.,* **2020;** *109*: 110354.

[12] Li CQ, Li C, Wang YF, Ren SQ, Wang HQ, Wang WW, Zhang JQ, Feng LH. Enhanced current collection of CdTe solar cells in the long wavelength region by co-evaporation deposition CdSexTe1-x films *Mater. Sci. Semicond. Process.*, **2021;** *121*: 105341.

[13] Yan SM, Fu HC, Zhang L, Dong YJ, Li WJ, Ouyang M, Zhang C. Conjugated polymer multilayer by in situ electrochemical polymerization for black-to-transmissive eletrochromism *Chem. Eng. J.*, **2020;** *406:* 126819.

[14] Yan SM, Fu HC, Dong YJ, Li WJ, Dai YY, Zhang C. Synthesis, electrochemistry and electrochromic properties of donor-acceptor conjugated polymers based on swivel-cruciform monomers with different central cores *Electrochim. Acta*, **2020;** *354*: 136672.

[15] Dai YY, Li WJ, Chen ZX, Zhu XG, Liu JL, Zhao RY, Wright DS, Noori A, Mousavi MF, Zhang C. An air-stable electrochromic conjugated microporous polymer as an emerging electrode material for hybrid energy storage systems *J. Mater. Chem. A,* **2019;** *7*(27):16397-16405.

[16] Dai YY, Li WJ, Zhao RY, Huang QD, Xu N, Yuan FY, Zhang C. Quadruple thiophene based electrochromic electrodeposited film as high performance hybrid energy storage system *Electrochim. Acta,* **2019**; *(318)*: 322-332.

[17] Qian L, Lv XJ, Ouyang M, Tameev A, Katin K, Maslov M, Bi Q, Huang CH, Zhu R, Zhang C. Fast switching properties and ion diffusion behavior of polytriphenylamine derivative with pendent ionic liquid unit *ACS Appl. Mater. Interfaces,* **2018**; *10*: 32404-32412.

[18] Shi YC, Chen QJ, Zheng JM, Xu CY. Electrochromism of substituted phthalate derivatives and outstanding performance of corresponding multicolor electrochromic devices *Electrochim. Acta*, **2020**; *341*: 136023-136029.

[19] Xu F, Wu X. M, Zheng JM, Xu CY. A new strategy to fabricate multicolor electrochromic device with UV-detecting performance based on TiO_2 and PProDOT-Me_2 *Org. Electron.*, **2019**; *65*: 8—14.

[20] Weng D, Li M, Zheng JM, Xu CY. High-performance complementary electrochromic device based on surface-confined tungsten oxide and solution-phase N-methyl-phenothiazine with full spectrum absorption *J. Mater. Sci.*, **2017**; *52*: 86—95.

[21] Guan SA, Wang WJ, Li BZ, Zheng JM, Xu CY. An inner-electropolymerization method for preparing electrochromic devices with various shapes and a large size *J. Mater. Chem. C.*, **2019**; *7*: 7520-7524.

[22] Li JJ, Guo QF, Lu Y, Nie GM. Polyindole vertical nanowire array based electrochromic-supercapacitor difunctional device for energy storage and utilization *Eur. Polym. J.*, **2019**; *113*: 29-35.

[23] Guo QF, Zhao XQ, Li ZY, Wang DB, Nie GM. A novel solid-state electrochromic supercapacitor with high energy storage capacity and cycle stability based on poly(5-formylindole)/WO_3 honeycombed porous nanocomposites *Chem. Eng. J.*, **2020**; *384*: 123370-123380.

[24] Guo QF, Li JJ, Zhang B, Nie GM, Wang DB. High-performance asymmetric electrochromic-supercapacitor device based on poly(indole-6-carboxylicacid)/TiO_2

nanocomposites *ACS Appl. Mater. Interfaces*, **2019**; *11*: 6491-6501.

[25] Nie GM, Wang L, Liu CL. High performance electrochromic devices based on a polyindole derivative, poly(1H-benzo[g]indole) *J. Mater. Chem. C*, **2015**; *3*: 11318-11325.

[26] Cui BB, Yao CJ, Yao JN, Zhong YW. Electropolymerized films as a molecular platform for volatile memory devices with two near-infrared outputs and long retention time *Chem. Sci.*, **2014;** *5*: 932-941.

[27] Cui BB, Mao ZP, Chen YX, Zhong YW, Yu G, Zhan CL, Yao JN. Tuning of resistive memory switching in electropolymerized metallopolymeric films *Chem. Sci*, **2015;** *6:* 1308-1315.

[28] Li ZJ, Shao JY, Wu SH, Zhong YW. Nanocrystalline Sb-doped SnO_2 films modified with cyclometalated ruthenium complexes for two-step electrochromism *Dalton Trans.*, **2019**; *48*: 2197-2205.

[29] Yao CJ., Zhong YW., Yao JN. Five-Stage Near-infrared electrochromism in electropolymerized films composed of alternating cyclometalated bisruthenium and bis-triarylamine segments *Inorg. Chem.* **2013;** *52*: 10000−10008.

[30] Tsukamoto T, Takada K, Sakamoto R, Matsuoka R, Toyoda R, Maeda H, Yagi T, Nishikawa M, Shinjo N, Amano S, Iokawa T, Ishibashi N, Oi T, Kanayama K, Kinugawa R, Koda Y, Komura T, Nakajima S, Fukuyama R, Fuse N, Mizui M, Miyasaka M, Yamashita Y, Tamada K, Zhang WX, Han RC, Liu WY, Tsubomura T, Nishihara H. Coordination nanosheets based on terpyridine‑zinc(II) complexes: as photoactive host materials *J. Am. Chem. Soc.*, **2017**, *139*, 5359-5366.

[31] Takada K, Sakamoto R, Yi ST, Katagiri T, Kambe T, Nishihara H. Electrochromic bis(terpyridine)metal complex nanosheets *J. Am. Chem. Soc.*, **2015**; *137*: 4681-4689.

[32] Bera MK, Ninomiya Y, Higuchi M. Stepwise introduction of three different transition metals in metallo-supramolecular polymer for quad-color elecrtochromism *Commun. Chem.*, **2021**; *4 (56)*, 1.

[33] Caceres G, Rojas V, Lopez S, Henriquez R, Grez P, Schrebler R, Herrera F, Pereyra CJ, Marotti RE, Navarrete E, Munoz E. Changes in the spectroelectrochemical properties of Copper(Ⅱ) hexacyanoferrate(Ⅲ) during electrochemical insertion of alkaline ions *J Solid State Electrochem*, **2021**; *25*: 1881-1888.

[34] Sakamoto R, Hoshiko K, Liu Q, Yagi T, Nagayama T, Kusaka S, Tsuchiya M, Kitagawa Y, Wong WY, Nishihara H. A photofunctional bottom-up bis(dipyrrinato)zinc(II) complex nanosheet *Nat. Commun.*, **2015**, *6*, 1.

[35] Aoki R, Toyoda R, Kogel JF, Sakamoto R, Kumar J, Kitagawa Y, Harano K, Kawai T, Nishihara H. Bis(dipyrrinato)zinc(II) Complex chiroptical wires: exfoliation into single strands and intensification of circularly polarized luminescence *J. Am. Chem. Soc.*, **2017**; *139*: 16024-16027.

[36] Chernyshev A, Acharya U, Pfleger J, Trhlikova O, Zednik J, Vohlidal J. Iron (Ⅱ) metal-supramolecular polymers based on thieno[3,2-b]thiophene for electrochromic applications *Polymers*, **2021**; *13*: 362-377.

[37] Mondal S, Santra DC, Ninomiya Y, Yoshida T, Higuchi M. Dual-redox system of

448 metallo-supramolecular polymers for visible-to-near-IR modulable electrochromism
449 and durable device fabrication *ACS Appl. Mater. Interfaces,* **2020**; *12*: 58277-58286.
450 [38] Vila N, Walcarius A. Bis(terpyridine) iron(Ⅱ) functionalized vertically-oriented
451 nanostructured silica films: toward electrochromic *Materials Front. Chem.*, **2020**; *8*:
452 830.
453 [39] Ninomiya Y, Yoshida T, Higuchi M. Electrochromic Fe(Ⅱ)-based
454 metallo-supramolecular polymers: color modulation by spacer modification in
455 bisterpyridine ligand *Chem. Lett.*, **2020**; *49*: 1003-1005.
456 [40] Liu YR, Sakamoto R, Ho C, Nishihara H, Wong WY. Electrochromic
457 triphenylamine-based cobalt(ii) complex nanosheets *J. Mater. Chem. C*, **2019**; 7:
458 9159-9166.
459 [41] Kuai Y, Li WJ, Dong YJ, Wong WY, Yan SM, Dai YY, Zhang C. Multi-color
460 electrochromism from coordination nanosheets based on a terpyridine-Fe(ii) complex
461 *Dalton Trans.*, **2019**, *48*, 15121-15126.
462 [42] Huang DC, Wu JT, Fan YZ, Liou GS. Preparation and optoelectronic behaviours
463 of novel electrochromic devices based on triphenylamine-containing ambipolar
464 materials *J. Mater. Chem. C*, **2017**, *5*, 9370-9375.